



Fermi National Accelerator Laboratory

FERMILAB-Conf-90/28-E
[E-741/CDF]

Log(s) Physics Results from CDF*

The CDF Collaboration

presented by

Morris Binkley

*Fermi National Accelerator Laboratory
P. O. Box 500
Batavia, Illinois 60510*

November 8, 1989

* Published in the proceedings of the International Europhysics Conference on High Energy Physics, Madrid, Spain, September 6-13, 1989.



LOG(S) PHYSICS RESULTS FROM CDF

The CDF Collaboration: Argonne, Brandeis, Chicago, Fermilab, Frascati, Harvard, Illinois, KEK, LBL, Pennsylvania, Pisa, Purdue, Rockefeller, Rutgers, Texas A&M, Tsukuba, Wisconsin

Presented by Morris Binkley

The Collider Detector at Fermilab (CDF) is a large, azimuthally symmetric detector designed to study $\bar{p}p$ interactions at the Fermilab Tevatron Collider. Results are presented from data taken with a minimum bias trigger at $\sqrt{s} = 630$ and 1800GeV during the 1987 run. The topics include the current analysis of $dn/d\eta$ and some very preliminary results on short range pseudorapidity correlations and Bose-Einstein correlations.

1 Detector and Data Selection

The detector has been described in detail elsewhere [1]. The analyses reported in this paper made use of the 1.5 Tesla magnetic field and three subdetectors. A large superconducting solenoid produced the magnetic field which was parallel to the beam axis (i.e. z direction). The trigger used the beam-beam counter scintillator hodoscopes (BBC) that cover a range in pseudorapidity[2] of $3.24 \leq |\eta| \leq 5.90$. Tracking was done by two other subdetectors. The vertex time projection chamber (VTPC) consists of 16 half-modules that surround the beam pipe in the central region and cover a pseudorapidity range $|\eta| \leq 3.5$. The electrons drift in the axial (z) direction providing a measurement of track projections in the $y-z$ plane. The large axial drift chamber (CTC) lies just outside the VTPC. This chamber has small angle stereo and covers a pseudorapidity range $|\eta| \leq 1$. The CTC has excellent resolution in the $r-\phi$ view allowing a precision momentum measurement.

The "minimum bias" trigger required at least one hit in both the upstream and downstream BBC hodoscopes and was identical for all of the data sets. Depending on the analysis, additional offline cuts were made on the number of tracks in the VTPC, the z of the interaction vertex, and additional BBC data. These selection criteria were very efficient for non-diffractive inelastic events and moderately efficient for double diffractive events. However they rejected most single-diffractive events. The differences in efficiencies and effective cross-sections were very slight for the different data samples. Typical efficiencies and effective cross sections are shown in Table 1.

Paper published Proceedings European Physical Society, International Europhysics Conference on High Energy Physics, Madrid, Spain, September 6-13, 1989.

630 GeV	est. $\sigma(mb)$	efficiency
Non-diffractive	33.9 ± 3.7	0.931
Single-diffractive	10.0 ± 0.7	0.111
Double-diffractive	2.5 ± 0.6	0.572
Total σ_{eff}		34 ± 3 mb
1800 GeV	est. $\sigma(mb)$	efficiency
Non-diffractive	40.2 ± 6.9	0.961
Single-diffractive	15.0 ± 5.0	0.160
Double-diffractive	4.2 ± 1.0	0.573
Total σ_{eff}		43 ± 6

Table 1: Monte Carlo estimates of the acceptance of our trigger and event-selection criteria for various components of the total cross-section

2 Pseudorapidity Density $dN/d\eta$.

The $dN/d\eta$ analysis was done using the data from the VTPC with special care taken to include interactions with as few as 2 tracks. With the cuts used, there was a contamination in the data sample due to single beam interactions that was $\leq 2.0\%$ at 630 GeV and $\leq 0.2\%$ at 1800 GeV. Events with vertices too close to the inactive region between VTPC modules were not used. There were backgrounds due to extra tracks from decays, photon conversions, and secondary interactions. Corrections were made for the three significant backgrounds. These were photon conversions (1% at $\eta = 0$ to 10% at $\eta = 3.5$), neutral kaon decays ($2 - 3\% \pm 1\%$ at all η values), and dalitz decays of neutral pions (1% at all η values). Corrections for tracking efficiencies were made that included the effects of tracks lost due to two track resolution and the curling of low momentum tracks in the VTPC. After corrections, the following results were obtained.

$$(dN/d\eta)_{\eta=0} = 3.18 \pm 0.05 (stat) \pm 0.10 (sys) \text{ at } 630 \text{ GeV}$$

$$(dN/d\eta)_{\eta=0} = 3.95 \pm 0.02 (stat) \pm 0.13 (sys) \text{ at } 1800 \text{ GeV}$$

$$\frac{\langle dN/d\eta \rangle_{1800}}{\langle dN/d\eta \rangle_{630}} = 1.26 \pm 0.01 (stat) \pm 0.04 (sys)$$

A plot of the corrected $dN/d\eta$ versus η at the two energies and their ratio are shown in figure 1.

3 Bose-Einstein Correlations

Bose-Einstein correlations[3] are relevant when the dimensions of the source are very small compared to the distance between the source and the detector, i.e. the detector cannot distinguish the points of origin of two particles. If the particles are identical bosons (wave function symmetric under particle exchange) and the source is incoherent, the probability of finding particles close together in phase space is enhanced.

These results are very preliminary. For this study, tracks from the CTC were selected with $P_t > 0.4 \text{ GeV}$ and $|\eta| < 1$. In addition, the tracks had to satisfy the following criteria: an impact parameter with the beam axis of less than 0.5 cm, a z match with the VTPC vertex of better than 5.0 cm, at least 8 of 12 hits in a minimum of two axial superlayers, and at least 4 of 6 hits in a minimum of one stereo superlayer. The event was

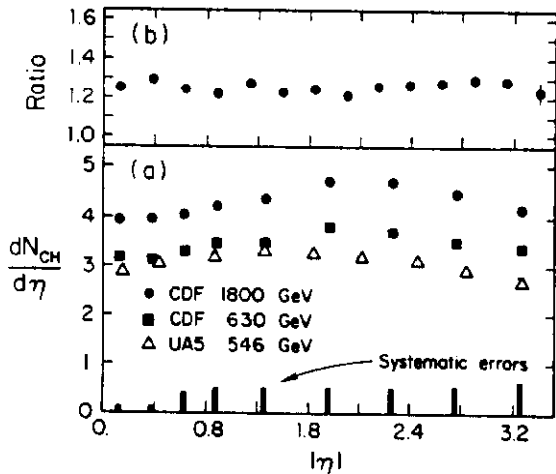


Figure 1: (a) The ratio of $dN/d\eta$ at 1800 GeV to that at 630 GeV. (b) $dN/d\eta$ measured by CDF at 1800 and 630 GeV, and by UA5 at 546 GeV. The size of the systematic error is indicated by bars at the bottom.

required to have at least three tracks in $|\eta| < 1$. All tracks were assumed to be pions for the analysis. The Kopylov [4] variables were used to study the correlations between particles 1 and 2.

$$\vec{q}_t = \frac{(\vec{P}_1 - \vec{P}_2) \times (\vec{P}_1 + \vec{P}_2)}{|\vec{P}_1 + \vec{P}_2|}$$

$$q_0 = |E_1 - E_2|$$

There are probability distributions $I(q_t, q_0)$ for particle pairs. $R(q_t)$ is the ratio of the distributions for like sign pairs to that for opposite sign pairs (or sometimes pairs randomized from different events) in a given q_0 interval. If the like sign pairs are identical bosons from an incoherent source, the ratio $R(q_t)$ can be related to the Fourier transform of the source distribution in the plane perpendicular to $\vec{P}_1 + \vec{P}_2$. If the source distribution is gaussian in this plane, then the ratio $R(q_t)$ has a component that is gaussian in q_t . This effect is strongly enhanced by using only particle pairs for which $q_0 < 100$ or 200 MeV . The ratio $R(q_t)$ should be constant if there are no correlations. In figure 2, the ratio $R(q_t)$ for $q_0 < 100 \text{ MeV}$ shows an enhancement at small values of q_t suggesting the presence of correlations. The following fit was made in order to parameterize the data.

$$R(q_t) = \gamma(1 + \delta q_t)(1 + \alpha e^{-\beta q_t^2})$$

where $\beta = R_s^2/\hbar^2 c^2$ with R_s being a measure of the source size. The value δ is used to isolate a small linear dependence on q_t not present in the theory. The first two bins

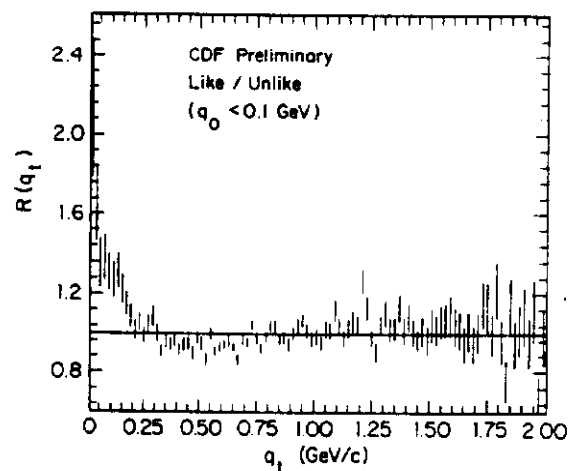


Figure 2: The ratio $R(q_t)$ of like sign pairs to opposite sign pairs vs q_t for pairs with $q_0 < 100 \text{ MeV}$ at 1800 GeV. Errors are statistical only.

\sqrt{s} GeV	q_0 MeV	γ	δ	β GeV^{-2}	α	R_b fm
1800 CDF	<100	0.90 ± 0.02	0.10 ± 0.02	25.1 ± 4.7	0.56 ± 0.07	0.99 ± 0.09
63 PP	<200	0.91 ± 0.02	0.03 ± 0.04	30.9 ± 3.2	0.67 ± 0.03	1.13 ± 0.04
63 $\bar{P}P$	<200	0.92 ± 0.03	-0.02 ± 0.06	28.3 ± 5.0	0.43 ± 0.05	1.03 ± 0.07
630 UA1	<200		0 fixed		0.25 ± 0.01	0.90 ± 0.03

Table 2: Results to fit of Bose-Einstein parameters for the ratio $R(q_i)$.

in q_i were excluded from the fits to the CDF data in order to eliminate any effects due to biases in the tracking algorithm for two nearby tracks. The results of the fit are shown in table 2 along with those for fits of other data [5][6]. Some other analyses have noted an increase of the source size with multiplicity. Due to limited statistics, there has been no attempt to determine the dependence on multiplicity in our data.

4 Pseudorapidity Correlations

This study involves charged particles seen in the VTPC and is also very preliminary. The specific event selection criteria for this analysis is that there be at least six VTPC tracks in the pseudorapidity range $|\eta| \leq 3$.

One and two charged particle densities are defined as follows.

$$\rho'(\eta) = \frac{1}{\sigma} \frac{d\sigma}{d\eta} = \frac{1}{N} \frac{\Delta n}{\Delta\eta}$$

$$\rho''(\eta_1, \eta_2) = \frac{1}{\sigma} \frac{d^2\sigma}{d\eta_1 d\eta_2} = \frac{1}{N} \frac{\Delta n_{12}}{\Delta\eta_1 \Delta\eta_2}$$

where Δn is the number of tracks in $\Delta\eta$; Δn_{12} is the number of pairs in $\Delta\eta_1$ and $\Delta\eta_2$; and N is the number of events. The two particle correlation function is defined as:

$$C(\eta_1, \eta_2) = \rho''(\eta_1, \eta_2) - \rho'(\eta_1)\rho'(\eta_2)$$

In addition there is a semi-inclusive correlation function:

$$C_M(\eta_1, \eta_2) = \rho''_M(\eta_1, \eta_2) - \rho'_M(\eta_1)\rho'_M(\eta_2)$$

where M refers to a fixed charge multiplicity or multiplicity range.

In order to get a feeling for what the various correlation functions mean, it is instructive to express the integral of the correlation function in terms of the event multiplicity n .

$$\int \rho'(\eta_1, \eta_2) d\eta_1 d\eta_2 = \langle n(n-1) \rangle$$

$$\int \rho'(\eta) d\eta = \langle n \rangle$$

$$\int C(\eta_1, \eta_2) d\eta_1 d\eta_2 = \langle n(n-1) \rangle - \langle n \rangle^2$$

Rewriting this in terms of the square of the second multiplicity moment $D_2^2 = \langle (n - \langle n \rangle)^2 \rangle = \langle n^2 \rangle - \langle n \rangle^2$ gives:

$$\int C(\eta_1, \eta_2) d\eta_1 d\eta_2 = D_2^2 - \langle n \rangle = f_2$$

If no correlations are present and the multiplicity distribution is Poisson, then $D_2^2 = \langle n \rangle$ and $f_2 = 0$. However it is well known that the multiplicity distribution is far from Poisson and that D_2^2 is much larger than $\langle n \rangle$ which means that f_2 is large. These "correlations" between events with different multiplicities cause both f_2 and $C(\eta_1, \eta_2)$ to be large at our center of mass energies. The increase of $C(\eta_1, \eta_2)$ with center of mass energy is mainly due to this effect. CDF data for the standard correlation function $C(\eta, 0)$ at $\sqrt{s} = 630$ GeV and 1800 GeV in figure 3 shows an increase with center of mass energy. Superimposed on the broad distribution that increases with energy are the "short range" correlations (described below) that cause an enhancement at $\eta_1 = \eta_2$.

When using the semi-inclusive correlation function $C_M(\eta_1, \eta_2)$ in the integral, D_2^2 approaches zero as the multiplicity interval M becomes small. The semi-inclusive

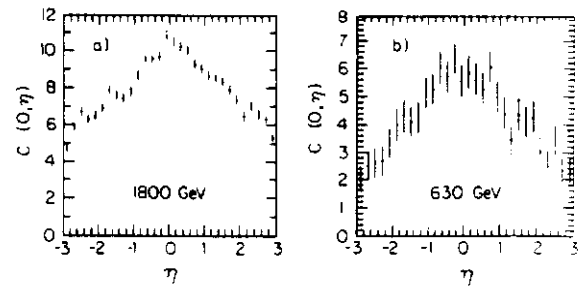


Figure 3: (a) The correlation function $C(0, \eta)$ vs η at 1800 GeV. (b) The same function $C(0, \eta)$ vs η at 630 GeV. Errors are statistical only.

function $C_M(\eta_1, \eta_2)$ is a measure of the dynamical correlations in $C(\eta_1, \eta_2)$ that occur within single events of definite multiplicity. They are usually referred to as "short range" correlations because $C_M(\eta_1, \eta_2)$ is sharply peaked at $\eta_1 = \eta_2$. The CDF data for the semi-inclusive correlation function $C_M(\eta, 0)$ at $\sqrt{s} = 1800 \text{ GeV}$ is shown in figure 4 for various multiplicity intervals.

Finally the semi-inclusive correlation function $C_M(\eta, \eta)$ was calculated for the various multiplicity intervals by averaging over $|\eta| < 1.5$. This result is shown in figure 5 along with data from UA5 [7]. There is good agreement with the UA5 data indicating little dependence on center of mass energy for this quantity.

5 Conclusions

The pseudorapidity density $dN/d\eta$ increases as a function of center of mass energy for $|\eta| < 3$ and the ratio of the densities for $\sqrt{s} = 1800 \text{ GeV}$ to $\sqrt{s} = 630 \text{ GeV}$ is

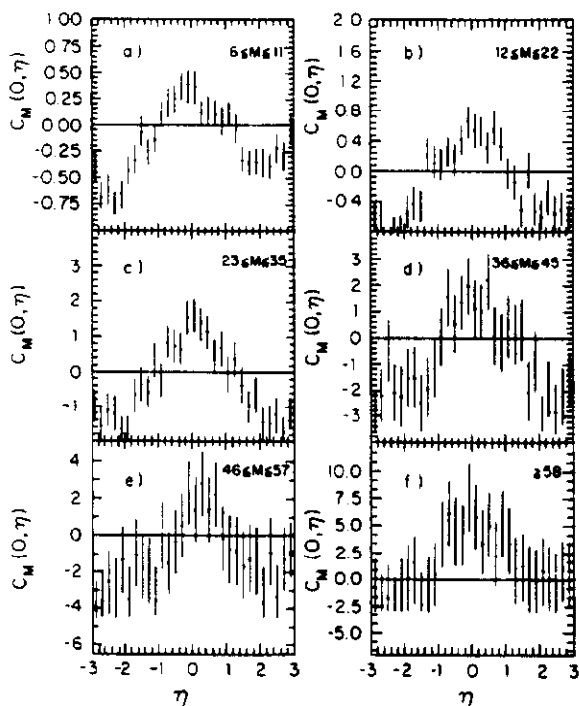


Figure 4: Semi-inclusive correlation function $C_M(0, \eta)$ vs η for different multiplicity intervals M at 1800 GeV . (a) $6 \leq M \leq 11$, (b) $12 \leq M \leq 22$, (c) $23 \leq M \leq 35$, (d) $36 \leq M \leq 45$, (e) $46 \leq M \leq 57$, (f) $58 \leq M$. Errors are statistical only.

consistent with being constant as a function of η in the measured η interval. Bose-Einstein correlations are observed at $\sqrt{s} = 1800 \text{ GeV}$ between identical pions with a measured source radius that is in agreement with previous results at lower center of mass energy. Inclusive two particle pseudorapidity correlations increase as expected with \sqrt{s} . The size of the short range two particle correlations at $\sqrt{s} = 1800 \text{ GeV}$ increases with increasing multiplicity and is consistent with no dependence on center of mass energy.

References

- [1] F. Abe et al., CDF Collaboration, Nucl. Instr. and Meth. A271 (1988) 387.
- [2] Pseudorapidity is $\eta = -\log(\tan(\theta/2))$ where θ is the angle of the particle with the beam direction.
- [3] G. Goldhaber et al., Phys. Rev. 120 (1960) 300.
- [4] G.I. Kopylov, Phys. Letters 50B (1974) 472.
- [5] C. Albajar et al., UA1 Collaboration, Physics Letters 226B (1989) 410.
- [6] A. Breakstone et al., Phys. Letters 162B (1985) 400.
- [7] R. E. Ansorge et al., UA5 Collaboration, Z. Phys. C - Particles and Fields 37 (1988) 191.

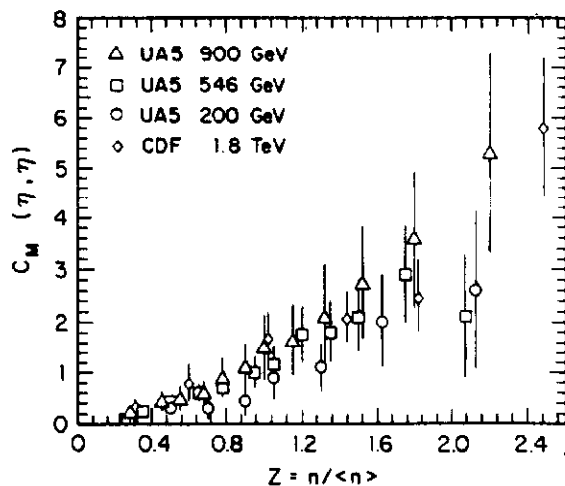


Figure 5: Semi-inclusive correlation function $C_M(\eta, \eta)$ averaged over $-1.5 \leq \eta \leq 1.5$ vs $z = n / \langle n \rangle$. The 1800 GeV data from CDF is plotted together with data from UA5 at 200, 546, and 900 GeV . Errors on the CDF data are statistical only.